

## ESI: In-situ Electron Microscopy Observation of the Redox Process in Plasmonic Heterogeneous-Photo-Sensitive Nanoparticles.

Diego Muraca<sup>a,†</sup>, Lucia B. Scaffardi<sup>b,c</sup>, Jesica M. J Santillán<sup>b</sup>, David Muñetón Arboleda<sup>b</sup>, Daniel C. Schinca<sup>b,c</sup> and Jefferson Bettini<sup>d</sup>

<sup>a</sup> Laboratório de Materiais e Dispositivos, Instituto de Física ‘Gleb Wataghin’, Universidade Estadual de Campinas, Campinas, Brazil

<sup>b</sup> Centro de Investigaciones Ópticas (CIOp) (CONICET La Plata-CIC-UNLP), Gonnet, La Plata, Buenos Aires, Argentina

<sup>c</sup> Departamento de Ciencias Básicas, Facultad de Ingeniería, UNLP, La Plata, Buenos Aires, Argentina

<sup>d</sup> Electron Microscopy Laboratory, Brazilian National Nanotechnology Laboratory/CNPEM.

### Movies Description

Movie 01: Selected parts of original movie with 29 frames per seconds where different events mentioned on the manuscript occur\*. Movie duration: 33 seconds. This Movie shows in-situ transmission electron microscopy experiments with three pre-existing *Ag*-NPs and between them *AgCl*. During this movie it can be observed how the amorphous phase of *AgCl* is reduced, the formation of crystalline *AgCl*, the formation, movement and dissolution of small NPs on the *AgCl*, the crystalline *AgCl* phase transformation and the dissolution of one pre-existing *Ag* NP.

Movie 02: Selected parts of original movie with 29 frames per second where different events mentioned on the manuscript occur\*. Movie duration: 41 seconds. This movie shows in-situ transmission electron microscopy experiments with three pre-existing *Ag*-NPs and between them *AgCl*. During this movie it can be observed how the amorphous phase of *AgCl* is reduced, the formation of crystalline *AgCl*, the formation and dissolution of small NPs on the *AgCl* and the dissolution of one pre-existing *Ag* NP at the left. At 820 s the magnification was increased allowing seeing in more detail the crystalline *AgCl* phase transformation. Edges and kinks movement are also observable at the end of the reaction.

Movie 03: Movie with 29 frames per second. Movie duration\*, 38 seconds. This movie shows in-situ transmission electron microscopy experiments with four pre-existing *Ag*-NPs and the presence of *AgCl*. Three of them in contact with *AgCl*. During this movie it can be observed the dissolution of small pre-existing NPs in contact with on the *AgCl* while the one that is not in contact prevails.

\*Original TEM movies were acquired with 160 frames per seconds

Movie 04: Different STEM images reconstructed on a film. Movie duration: 7 seconds

### Supplementary Information

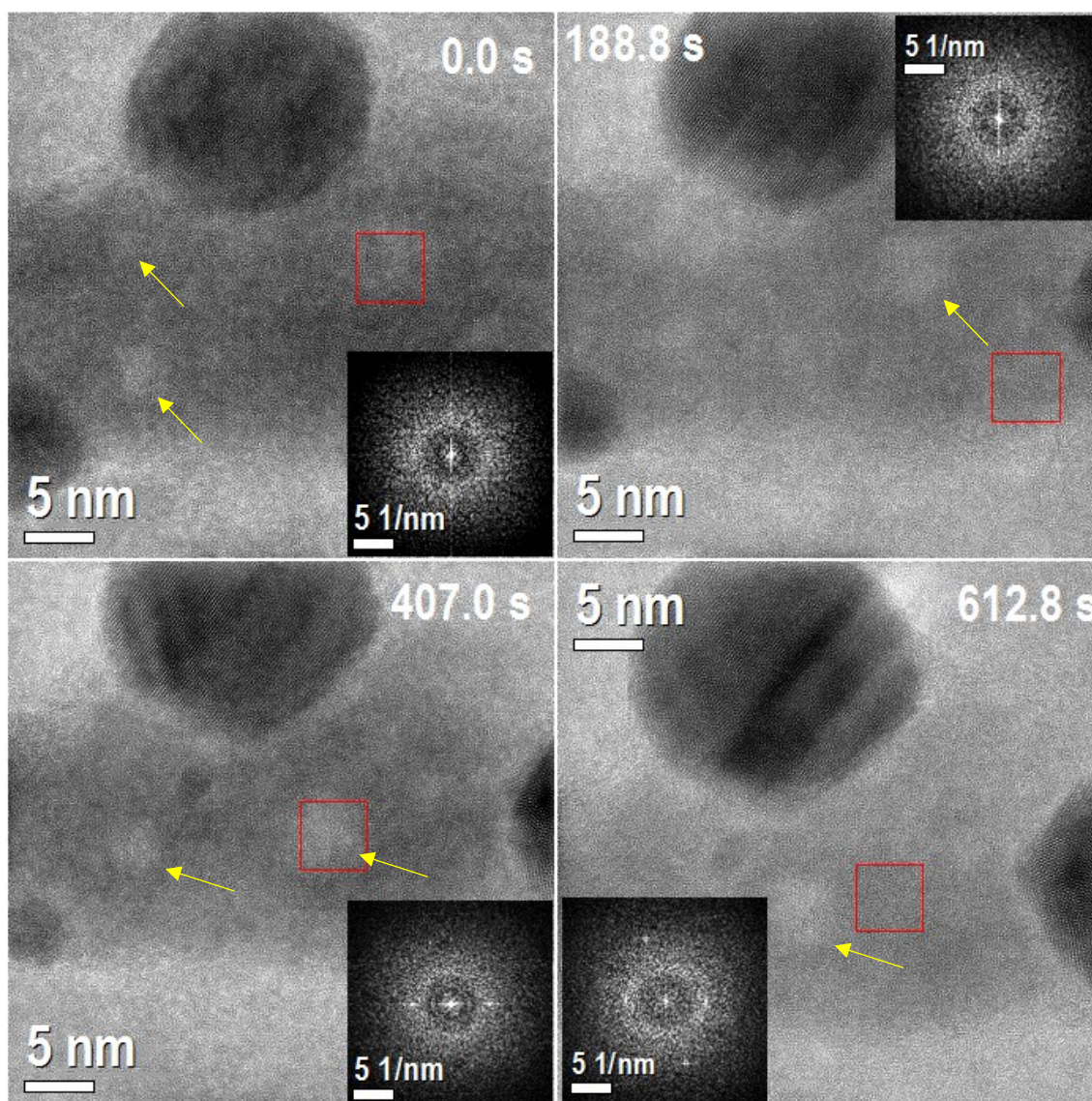


**Fig. S1** This figure shows different times of Movie 2 at initial stage of the reaction with 3 *Ag* NPs and a between them *AgCl*-NP. The corresponding times are shown on each image. Darkest contrasts correspond to the *Ag*-NP, whereas less dark contrast corresponds to the *AgCl* phase. The insets inside of each figure correspond to a fast Fourier transform (FFT) of the region denoted by the red box for each corresponding time. The FFTs show weak spots indicating the existence of a minority crystalline phase with the majority amorphous phase. Two nanometer-sized “nanobubbles” (brighter contrast, yellow arrows) are present on the system within the *AgCl*-NP.

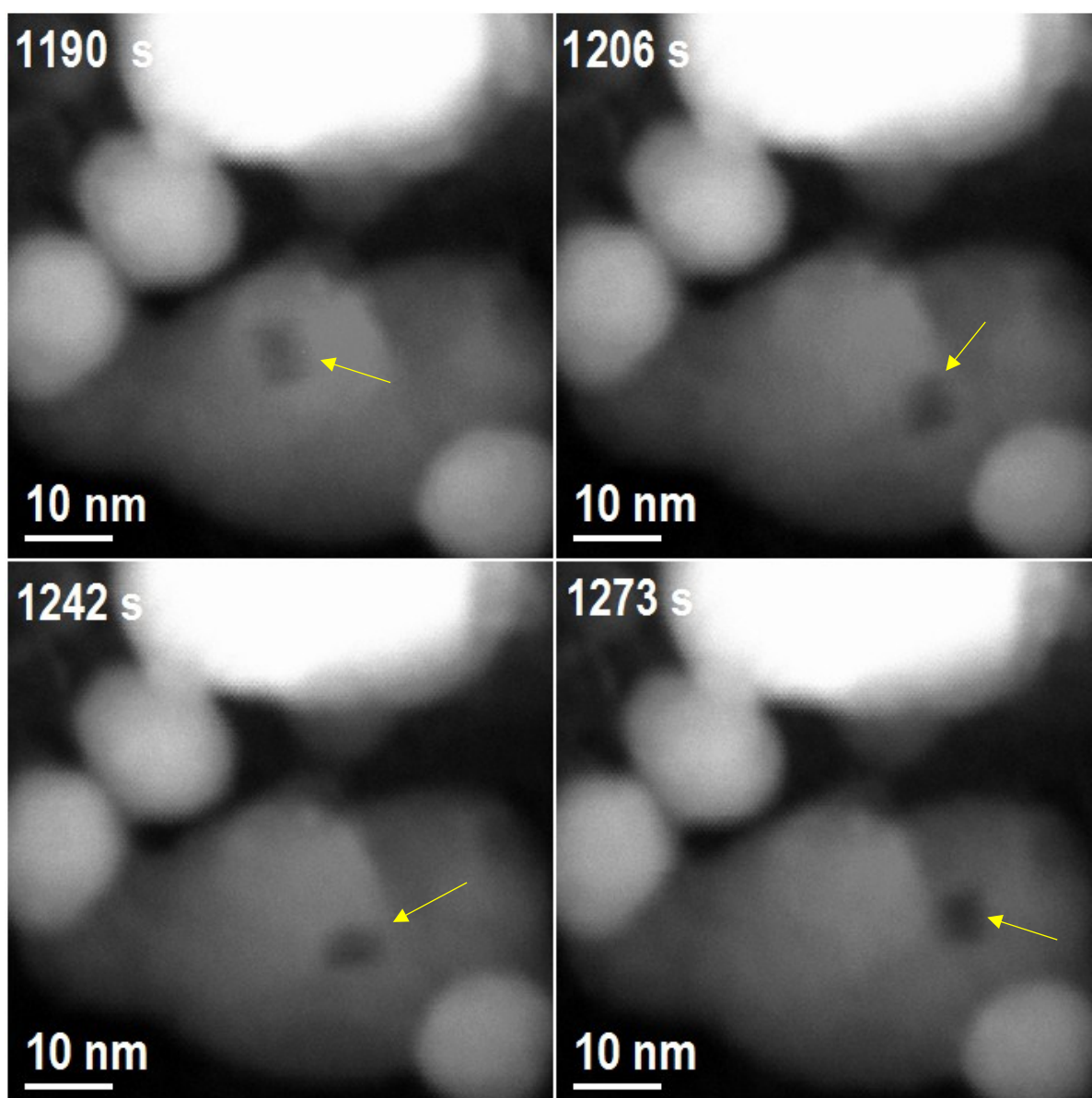


**Fig. S2** Different times of Movie 4, showing images during scanning transmission electron microscopy (STEM) acquisition, when in-situ energy dispersive spectroscopy experiments were performed. The corresponding times are shown on each image. Brighter contrasts correspond to the *Ag*-NP, whereas less bright contrast corresponds to the *AgCl* phase. Five *Ag*-NP in total are observed, four in the outer parts, and the last one superimposed to *AgCl*. The last one is in contact and surrounded by *AgCl* and between the others. A small nanobubble appears inside the *AgCl*-NP (small sphere with dark contrast in the *AgCl* phase) and was registered at 4 different places at the different times shown. The silver NP surrounded by *AgCl* starts to dissolve gradually. Yellow arrows indicate places with presence of nanobubbles.

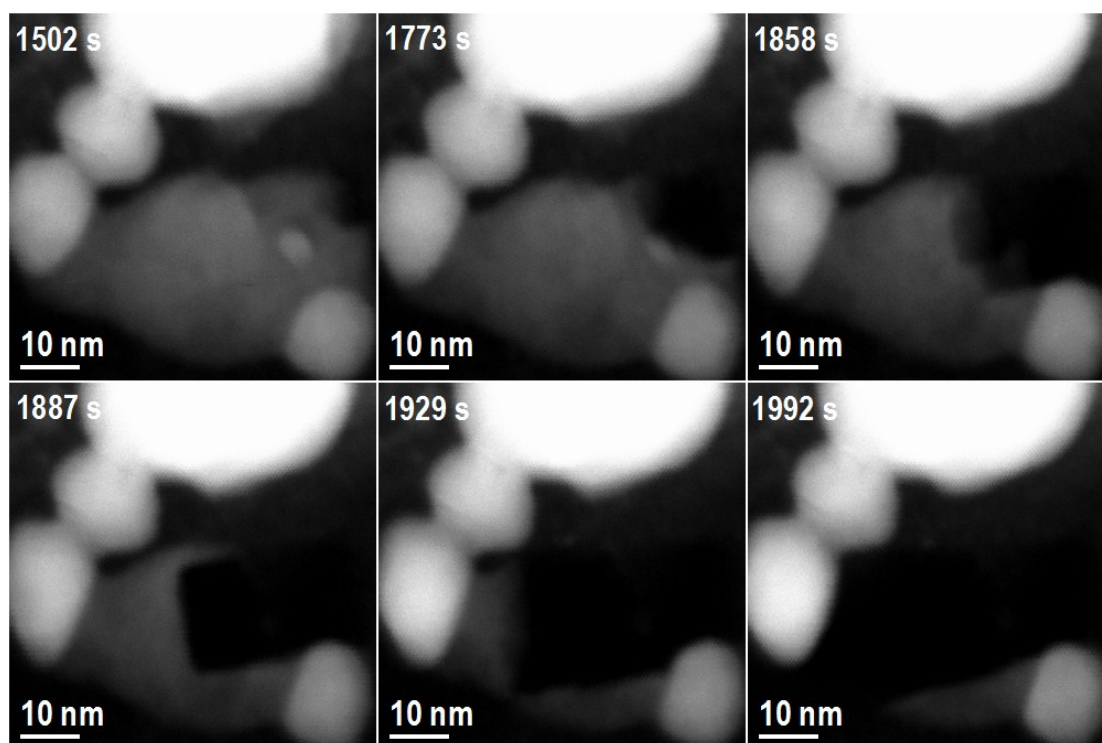


**Fig. S3** The images correspond to different times of Movie 4 during scanning transmission electron microscopy (STEM) acquisition, when in-situ energy dispersive spectroscopy experiments were performed. The corresponding times are shown on each image. The last place where a nanobubble was registered (see last panel 1273 s) a small silver NP “nucleates” (small sphere with bright contrast in the *AgCl* phase). Simultaneously, a dark contrast begins to increase on the upper right edge with a square shape, related to the *AgCl* crystalline shell structure of the AgCl NP.

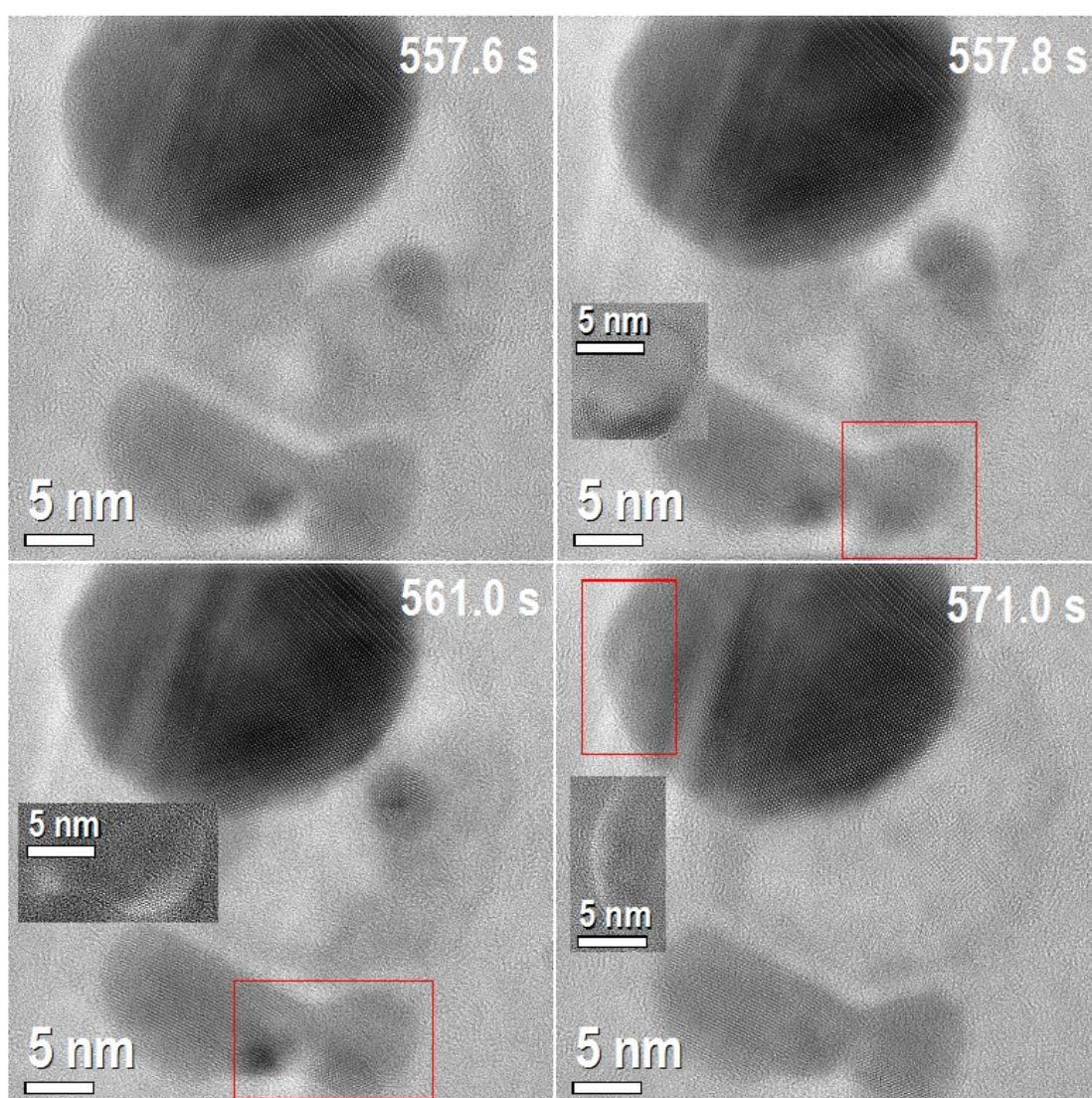
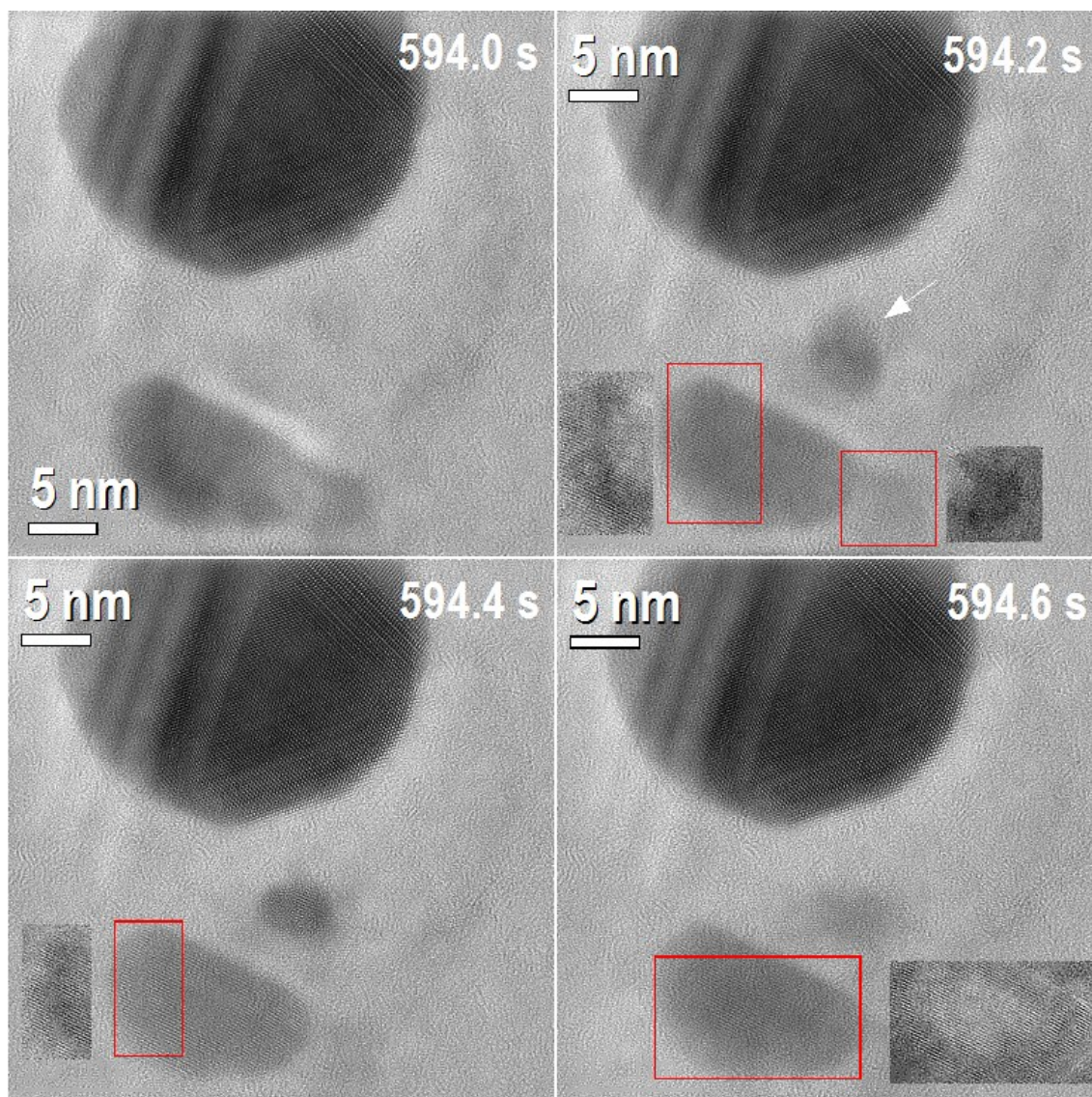


**Fig. S4** Time sequence of the reaction for 13.4 seconds of the Movie 1. The corresponding times are shown on each image. 557.6 s: shows the initial condition of



the time sequence with three original silver NPs and a small silver nanoparticle formed on the  $AgCl$ , between the  $Ag$  NPs. 557.8 s: small formed nanoparticle increases its size, dark contrast on the small box evidence mass loss from the  $Ag$ -NP at the bottom right denoted by a red box. The mass difference was obtained by subtraction of figure at 557.6 s from 557.8 s. 561.0 s: small formed nanoparticle reduces its size, bright contrast on the small box evidence mass gain on the  $Ag$ -NP at the bottom right denoted by the red box. The mass difference was obtained by subtraction of figure at 557.8 s from 561.0 s. 561.0 s: small formed nanoparticle is fully dissolved, bright contrast on the small box evidence mass gain on the  $Ag$ -NP at the top left denoted by the red box. The mass difference was obtained by subtraction of figure at 571.0 s from 561.0 s.

**Fig. S5** Time sequence of the reaction for 0.6 seconds of the Movie 1. The corresponding times are shown on each image. 594.0 s: initial condition of the time sequence with two original silver NPs and  $AgCl$  between the  $Ag$  NPs. 594.2 s: small  $Ag$ -NP is formed, dark contrast on the small boxes evidences mass loss from the  $Ag$ -NP at the bottom, the places are denoted by the red boxes. The mass difference was obtained by subtraction of figure at 594.0 s from 594.2 s. 594.4 s: the small previously formed nanoparticle reduces its size, bright contrast on the small box evidence mass gain on the  $Ag$ -NP at the bottom denoted by red box. The mass difference was obtained by subtraction of figure at 594.4 s from 594.2 s. 594.6 s: the formed nanoparticle is fully dissolved, bright contrast on the small box evidences mass gain on the  $Ag$ -NP at the bottom denoted by the red box. The mass difference was obtained by subtraction of figure at 594.6 s from 594.4 s.

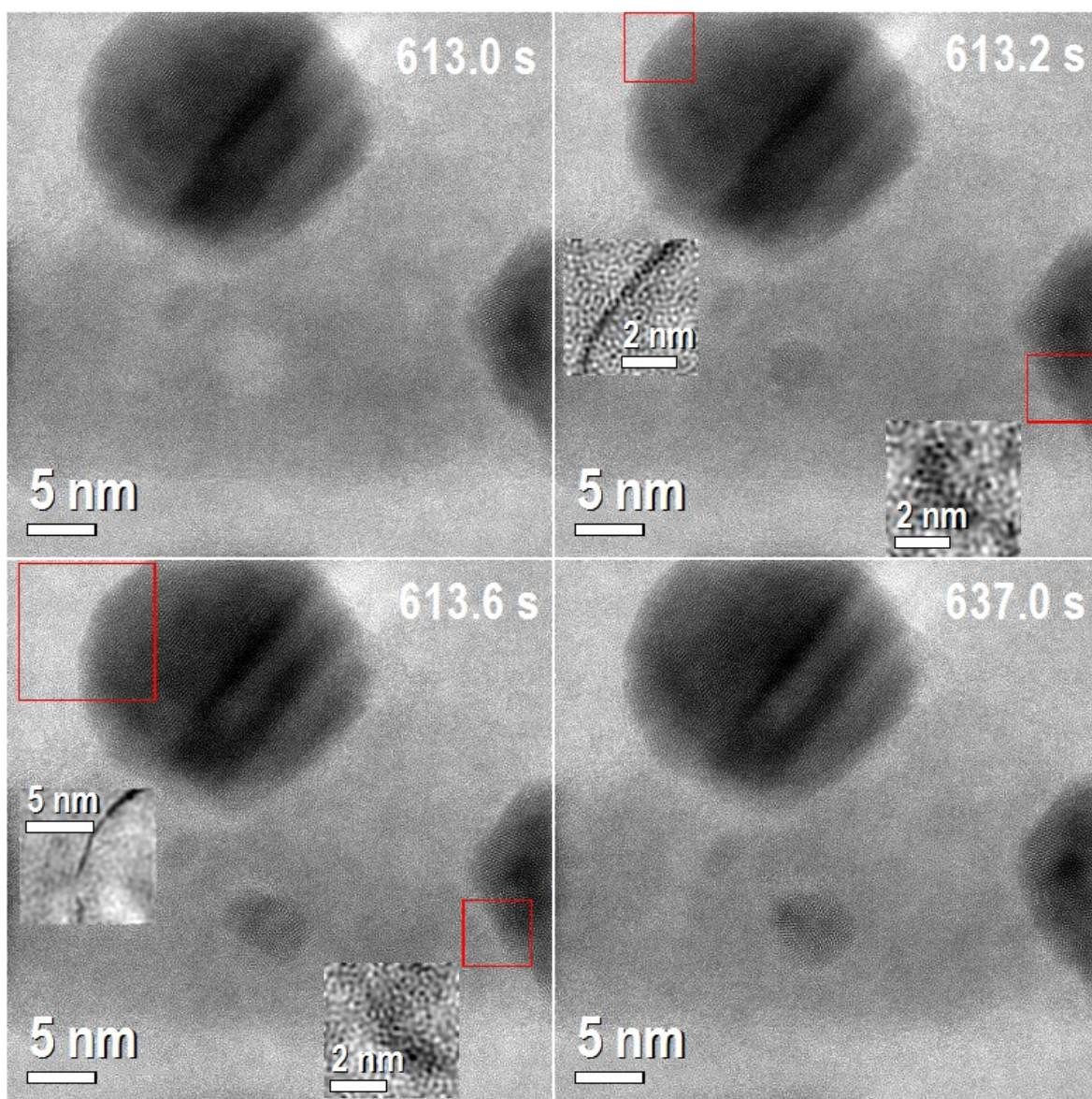


**Fig. S6** Time sequence of the reaction for 24.0 seconds of the Movie 2. The corresponding times are shown on each image. 613.0 s: shows the initial condition of the time sequence with two original silver NPs and *AgCl* between the *Ag* NPs. A small nanobubble of 3.5 nm can be noticed by bright contrast in the *AgCl*. 613.2 s: small silver NP of 3.5 nm is formed between the other *Ag*-NPs on the place where the nanobubble was present before, dark contrast on the small boxes evidences mass loss on specific places (denoted by red boxes) of the *Ag*-NPs. The mass difference was obtained by subtraction of figure at 613.0 s and at 613.2 s. 613.6 s: small formed nanoparticle increases its size, dark contrast on the small box evidences mass loss on the *Ag*-NPs. The



places are denoted by red boxes. The mass difference was obtained by subtraction of figure at 613.0 s and at 613.6 s. 537.0 s: Final stage of this sequence with a silver nanoparticle formed and before its final dissolution.

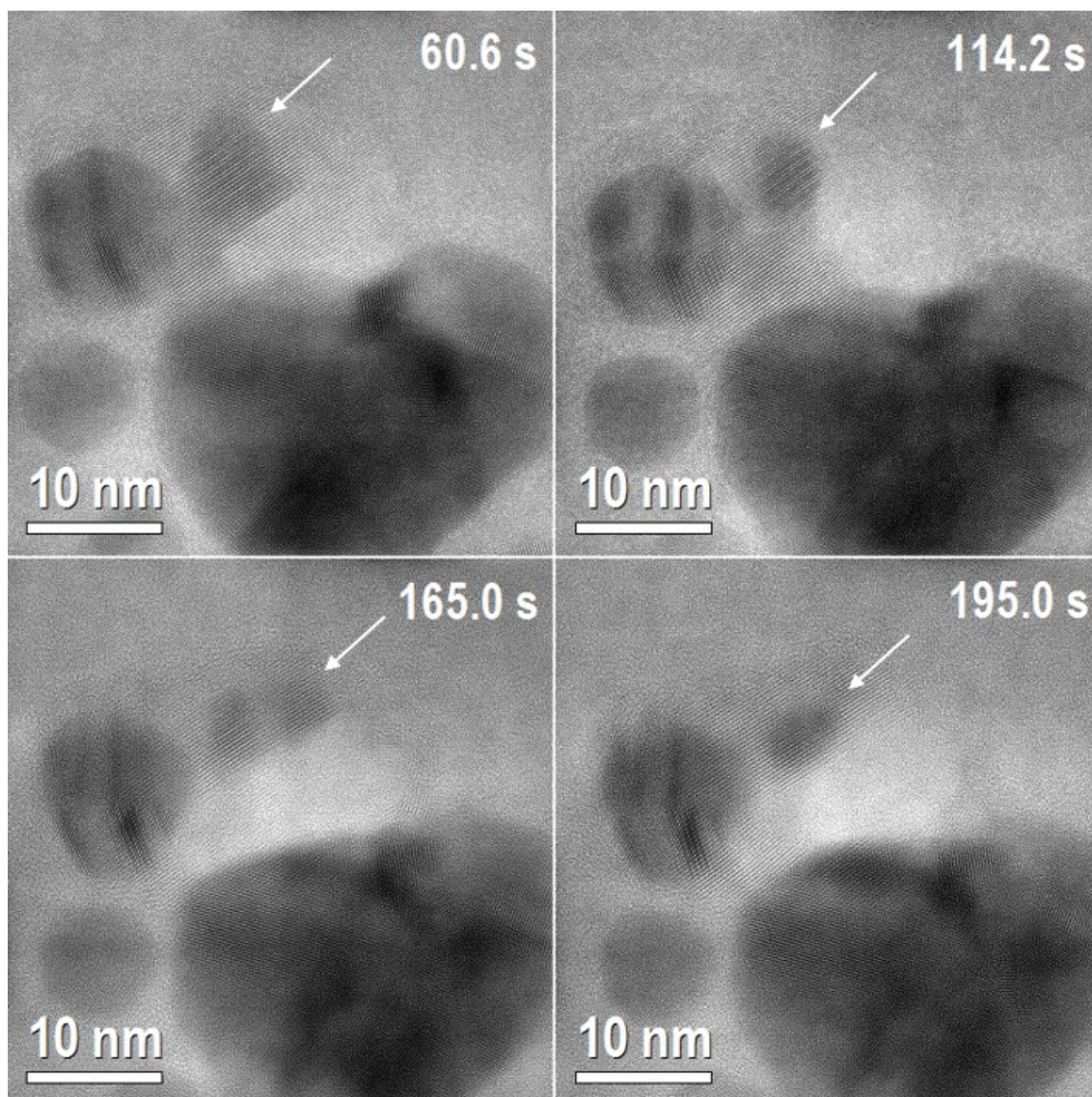


**Fig. S7** Time sequence of the reaction for 135 seconds of the Movie 3. The corresponding times are shown on each image. The *Ag*-NP indicated by the white arrows has the shape defined by the *AgCl* planes movements during the dissolution process. 114.2 s: The *Ag*-NP is compressed when *AgCl* planes are reduced. 165.0 s: The *Ag*-NP is stretched when the *AgCl* planes grow. 195.0 s The *Ag*-NP shows mass loss and the bigger NP increases its size.

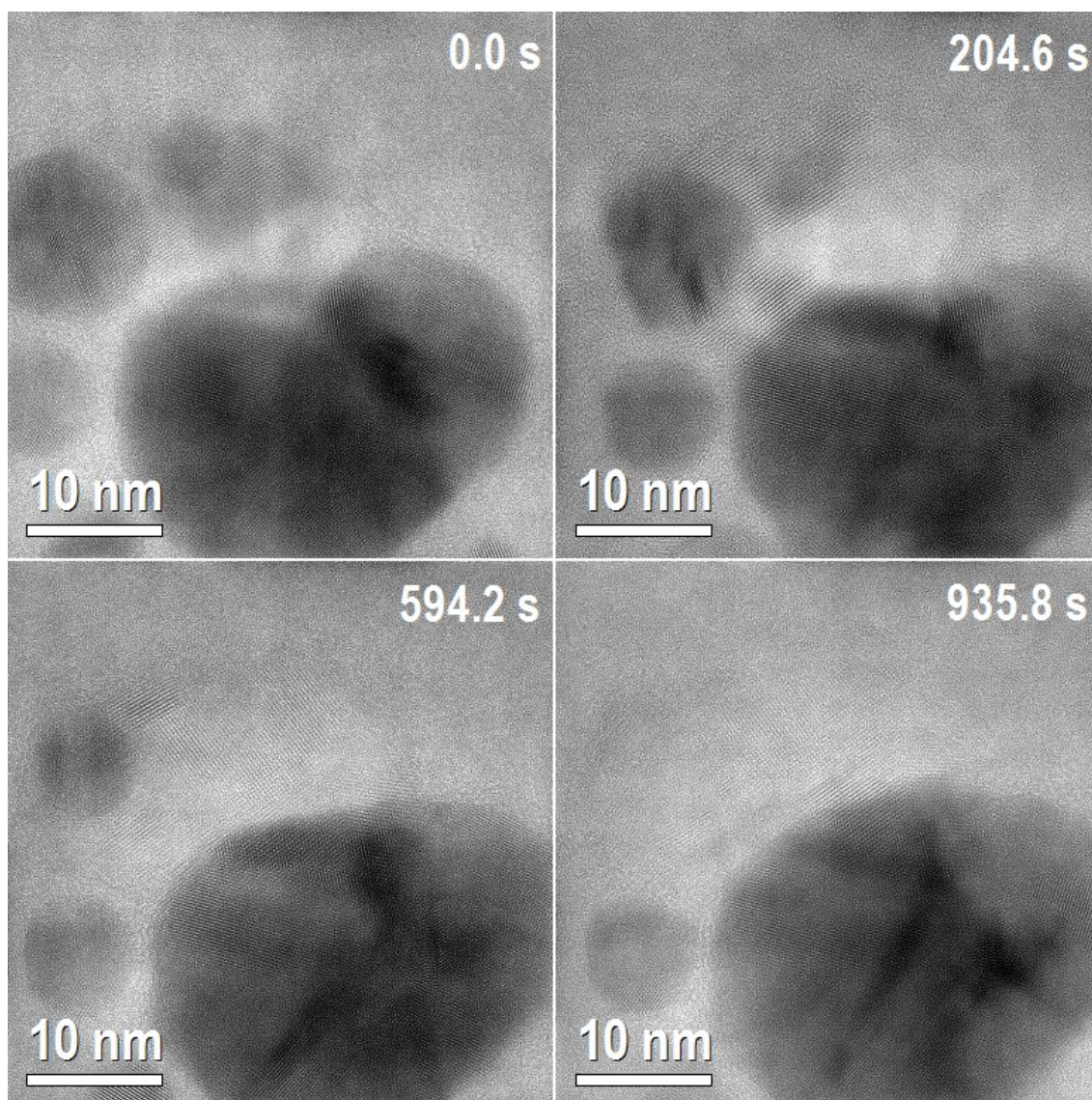


**Fig. S8** Shows a time sequence of the reaction for 935.8 seconds of the Movie 3. The corresponding times are shown on each image. 0.0 s: shows the initial condition of the time sequence with four silver NPs and *AgCl* in contact with three *Ag* NPs. 204.6 s: The *Ag*-NP in the upper part, which is in contact with the *AgCl* NPs, is dissolved during the reaction while the *AgCl* lattice evolves. 594.2 s: One of the *Ag*-NP is fully dissolved and the size of another *Ag* NP in contact with *AgCl* is also reduced. 935.8 s: Both smaller NPs in contact with *AgCl* were fully dissolved. The biggest one increased its size and became more spherical. The *Ag* NP that was not in contact with *AgCl* preserved its size.

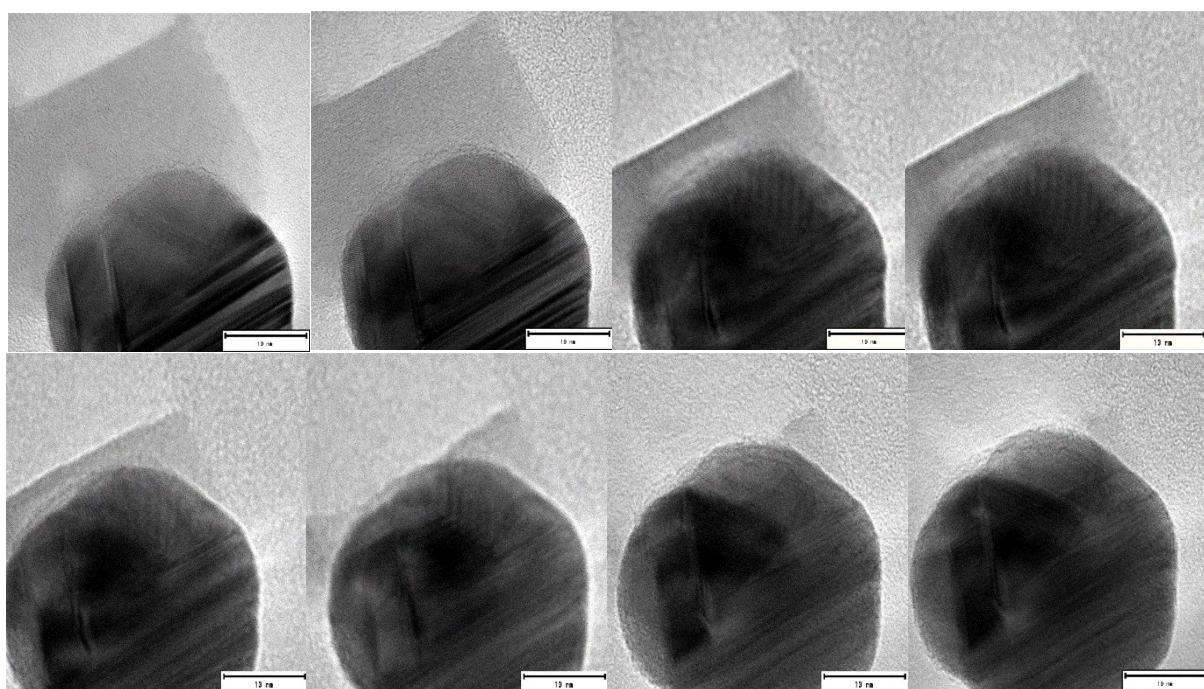


**Fig. S9:** Image sequence of a single silver nanoparticle with silver chloride.

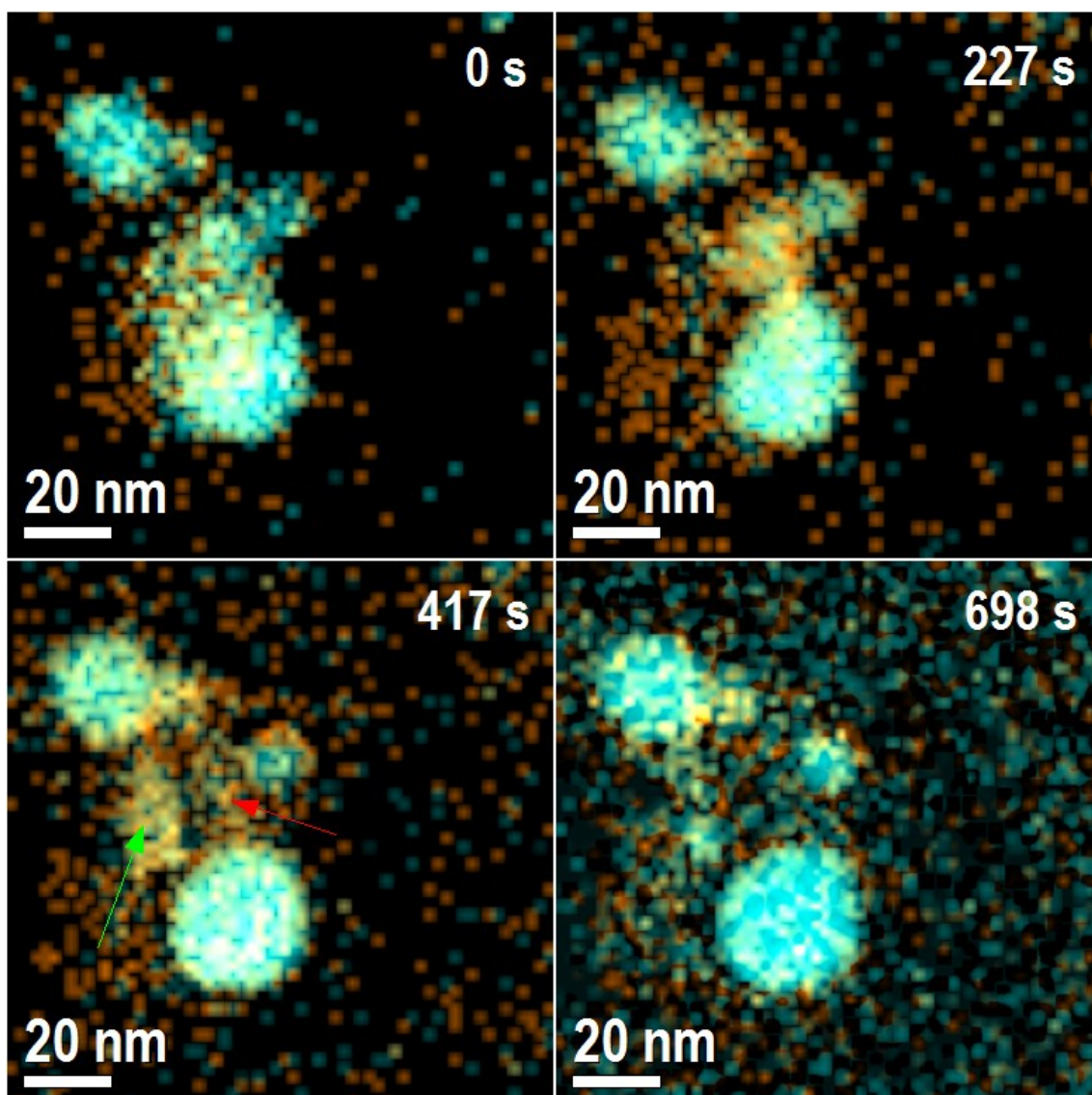


**Fig. S10.** In-situ energy dispersive spectroscopy showing composition variation for 698 seconds. Cyan color corresponds to the silver L-edge, and orange color corresponds to the chlorine K-edge. Figure shows the flux of silver mass (cyan color) from one place to others. Some of the silver NPs increase their sizes during the reaction, and at the same time, the atomic amount of silver and chlorine atoms (orange color) concentration is reduced on the silver chloride phase. At 417 s, a new NP is formed on a new place, denoted by a green arrow. The atoms forming the new NP come from a place between the biggest ones (see 227 s), denoted by a red arrow. Silver and chlorine relative atomic concentration are reported in Table S1. Global silver relative atomic percentage increases about 1.5 times, whereas chlorine is reduced in the same value.

**Table S1:** Global atomic composition evolution obtained by means of EDS of sample Figure S9.

Sample Figure S16		
Ag (% at.)	Cl (% at.)	Time (s)
76±1.2	24±2.6	0
82±1.3	18±3.5	227
85±1.1	15±3.1	417
90±0.7	10±2.2	698

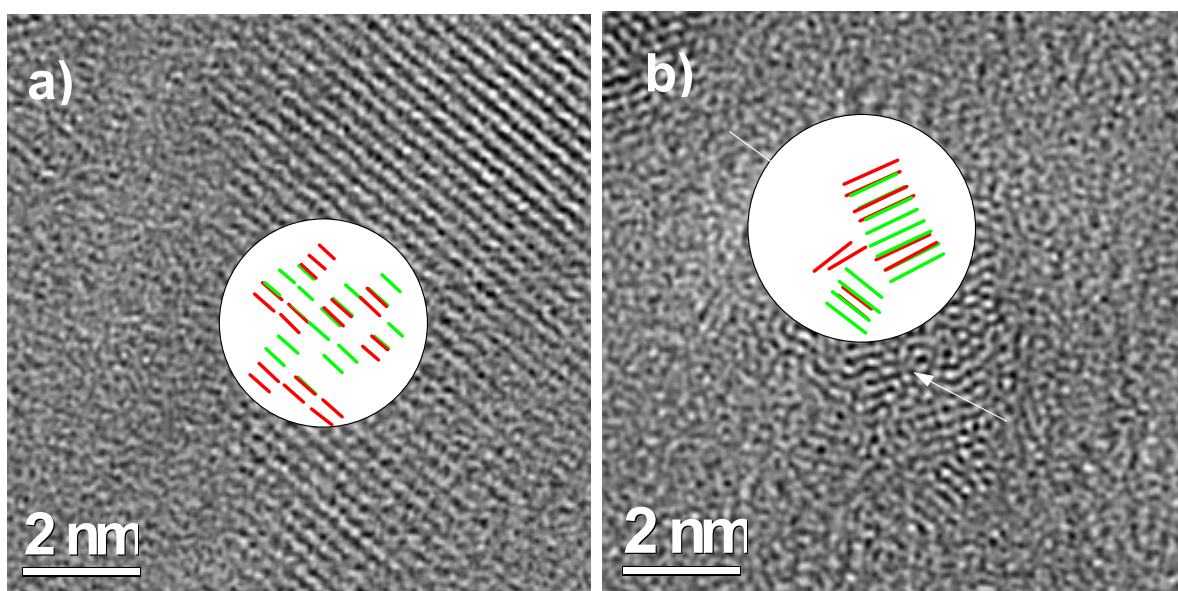


**Fig. S11.** a) Details of the inverse FFT with the background removed of Fig. 4 d), b) more detail of the inverse FFT with the background removed of Fig. 5 d),

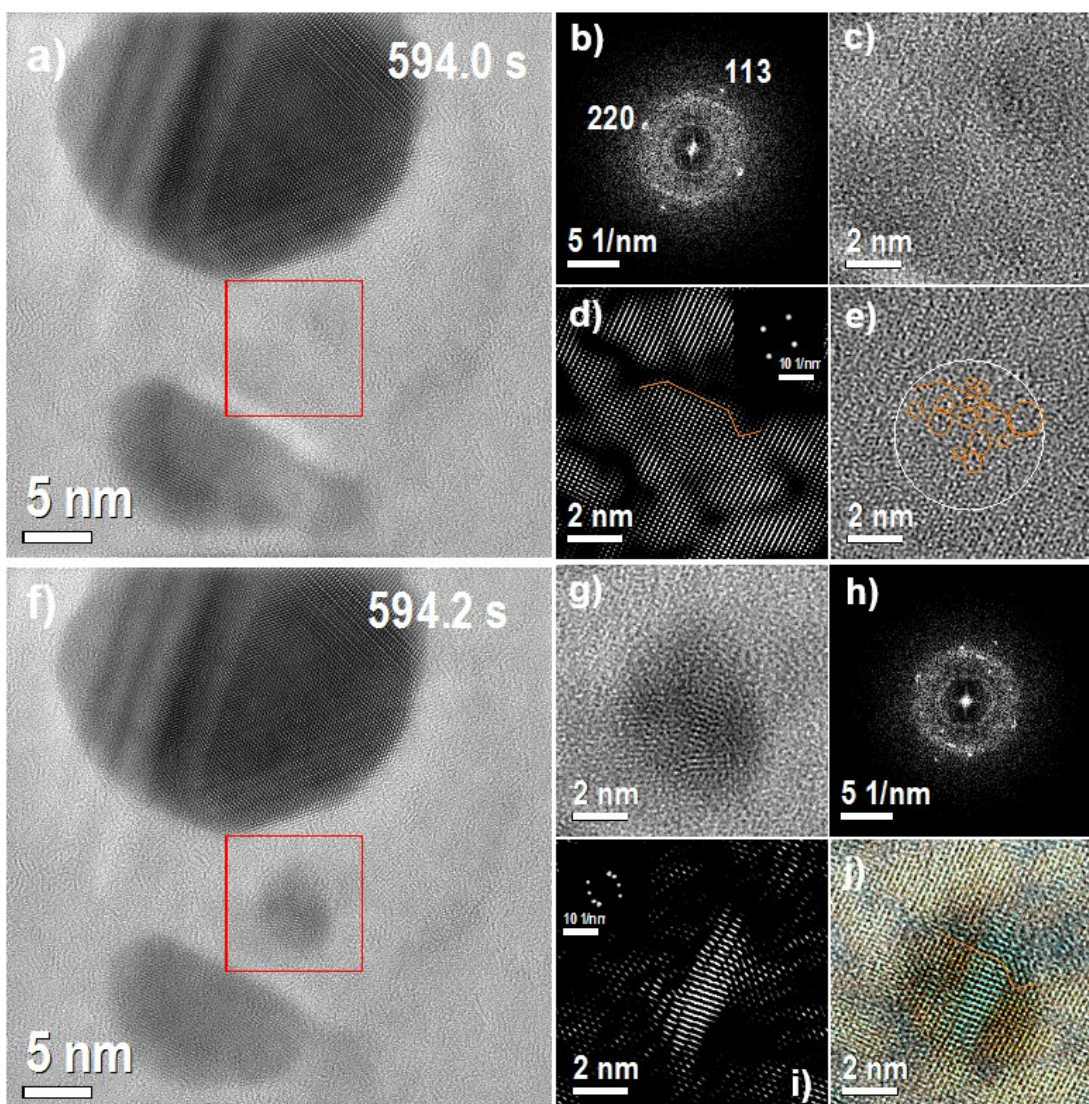


**Fig. S12.** This figure corresponds to the nucleation of *Ag*-NP shown in Figure S5. From left to right, and top to bottom: a) Image before the nucleation of *Ag*-NP with the region where the nucleation occurs denoted by a red box (594.0 s), b) the FFT of the region denoted by red box, c) the inverse FFT of the same region (2x zoom in), d) the inverse FFT with masks applied in the spots (200) and (113), e) inverse FFT with the background removed, f) image with the *Ag*-NP nucleated and same region marked by red box, g) image marked by red box with 2x zoom in (594.2 s), h) FFT of the region denoted by red box (594.2.8 s), i) inverse FFT image obtained with masks applied in the spots corresponding to the *Ag*-NP planes and j) composite image with image g), image d colored orange and image i) colored blue.

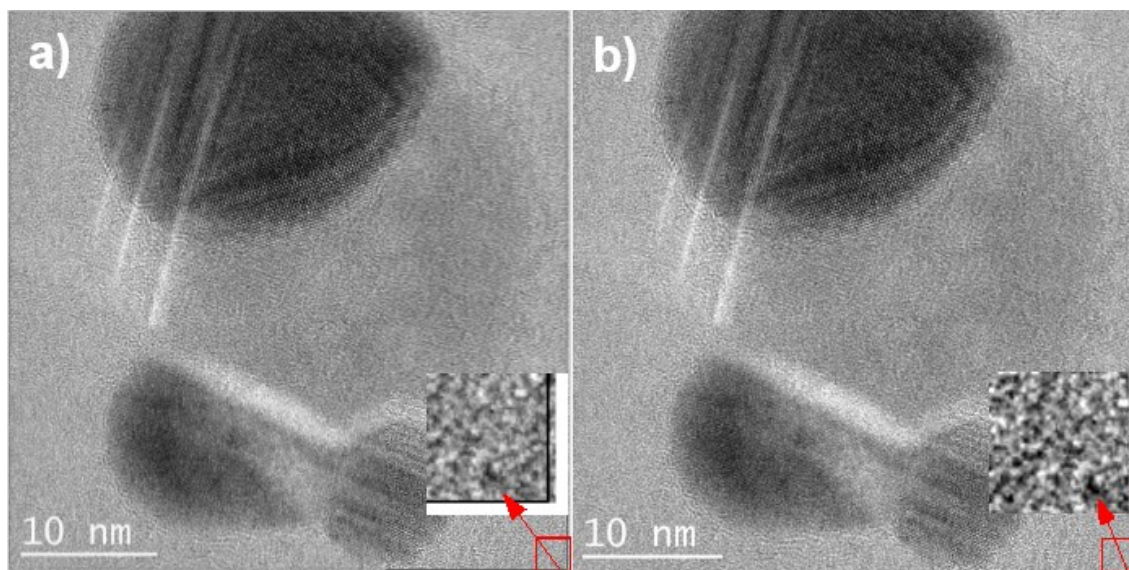
Fig. S10 shows a more detailed analysis of the nucleation process shown previously in Fig. S5. Fig. S10, b) (FFT from the red box) shows two spots corresponding to (220) and close to (113)  $AgCl$  planes with an angle of 90 degrees between them, the (220) has 0.199 nm and (113) has 0.162 nm distances.  $AgCl$  fcc-structure has neither zone axis with 90 degrees between the (220, 0.199 nm) and (113, 0.17 nm)  $AgCl$  planes. This fact can explain the stress measured in the (113) form FFT in the Fig. S10, b). Fig. S10, c) shows the Inverse FFT from Figure b) with 2x zoom in. Fig. S10, d) was obtained applying a mask in the (113) and (220) spots in the FFT of the image S11. Afterwards the contrast and brightness were adjusted to 0.9 and 0.3 working as an intensity filter. Figure S11, d) shows the formation of edges in the image obtained with the combination of (220) and (113)  $Ag$  planes. The orange circles in the Fig. S10 e) denote regions with a distance larger than 0.2 nm and smaller than 0.28 nm indicating a vacancy defect and stretched regions. So, the stressed (113) planes, vacancy defects and edges formation can create a region with some charge or field accumulation and attracts the  $Ag$  atoms to nucleate in this region. Planes corresponding to  $Ag$ -NP shown in Fig. S10, i) matches with the main regions of defects observed in figure e) as can be observed in the Fig. S10, j).

#### *Image Data Processing Details*

The frames movies were extracted using IrfanView software. The images were cropped to remove the edge of the software window. Supplementary Figure S11 shows an example of this process. The scale mark was replaced by the average local intensity using a specific script. Supplementary Figure S12 shows the result after this process. The amorphous information in the image was reduced using three-band pass filter combined with Gaussian function to smooth the edge of the masks. Supplementary Figure S13 shows the results after the band pass filters applied.

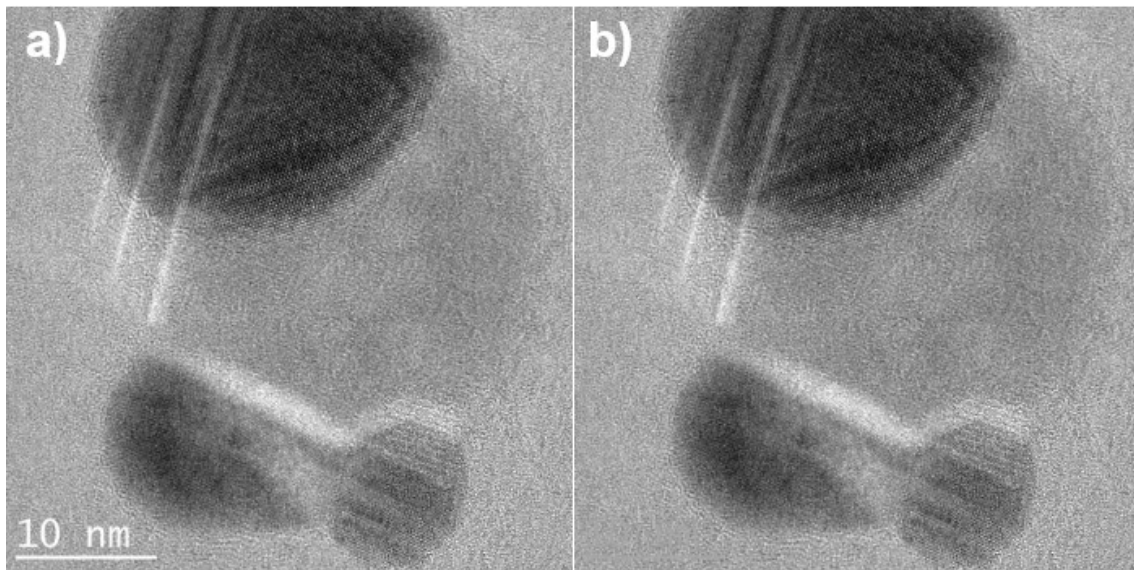


After the application of band pass filters, the high-resolution information became more accessible to observe. Finally, the images were recalibrated using the Ag-NP planes distances as references. A cross-correlation function using sequential alignment (no rigid alignment) was used to align the images of the movies. Afterwards, the scale marker and time was added outside the images. The movies were compiled by more than one original movie because of RAM issues. For example, Movie 1 is composed of three original movies. Therefore, the transition between two internal movies to



another was marked by black images and the time between them was considered as 5 seconds. Finally, the real time and scale were added to the image and the movies were assembled.

**Fig. S13.** a) original image extracted from the movie acquired from the screen computer



and b) image cropped to remove the edge of the software window.

**Fig. S14.** a) image with scale mark and b) image after the scale mark replaced by the average local intensity.

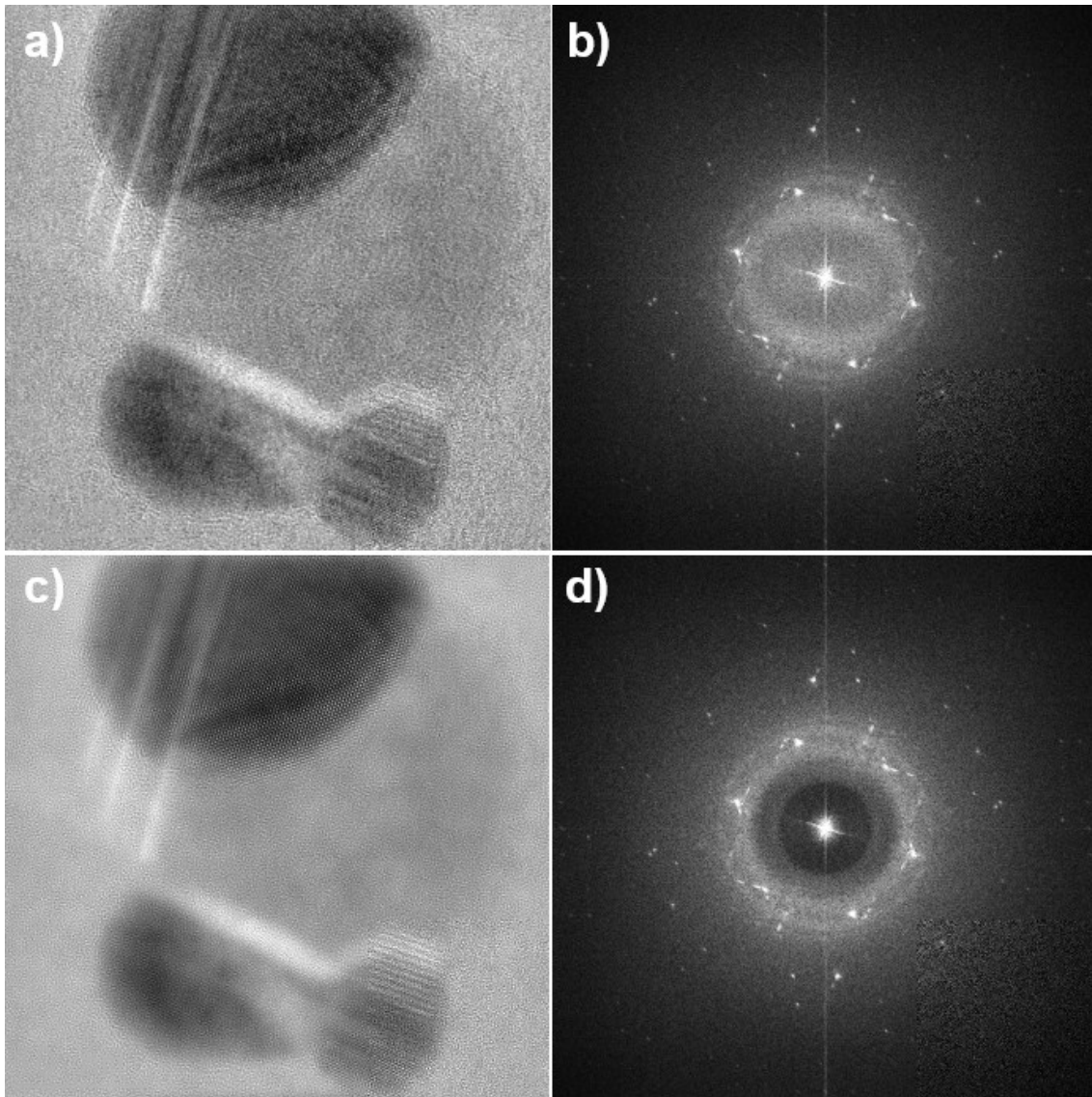


**Fig. S15.** a) image before the application of band pass filters, b) FFT of the image a), c) image after the application of band pass filters and d) the corresponding FFT of image c).

*The mass gain/loss image analysis process has the following steps:*

1. Normalize the two images (two consecutive images). We have also taken care to remove the “nucleates” Ag-NP before the normalization.
2. Cross-correlation to avoid any drift effect in the process. The cross-correlation was applied in the whole image and double-checked using a part of the image without any mass gain or loss.
3. Apply the subtraction between the two images.
4. Apply a low pass filter to increase the contrast, and the regions with mass gain or loss appear with good contrast. Sometimes the low pass filter was not used since the contrast of the regions after the subtraction can be observed easily, for example, figure S4. Fig. S15 shows the whole process applied in the construction of Figure 2 with the same regions highlighted by the red box and arrow. The figure displays the result for the three subtractions with the areas magnified two times shown in Fig. 2. As can be observed, the dark region (mass loss) in the second subtraction and white region (mass gain) in the third subtraction are identified without a significant effort. In the first subtraction, the area in the bottom is identified as the most significant region with dark contrast. Therefore, we noticed that the atoms that are involved with this new NP (nucleation and dissolution) correlate with at least two different and specific places (apart from the one denoted by an arrow), indicated by the red box (left edge in the upper Ag-NP and right edge in the bottom Ag-NP).

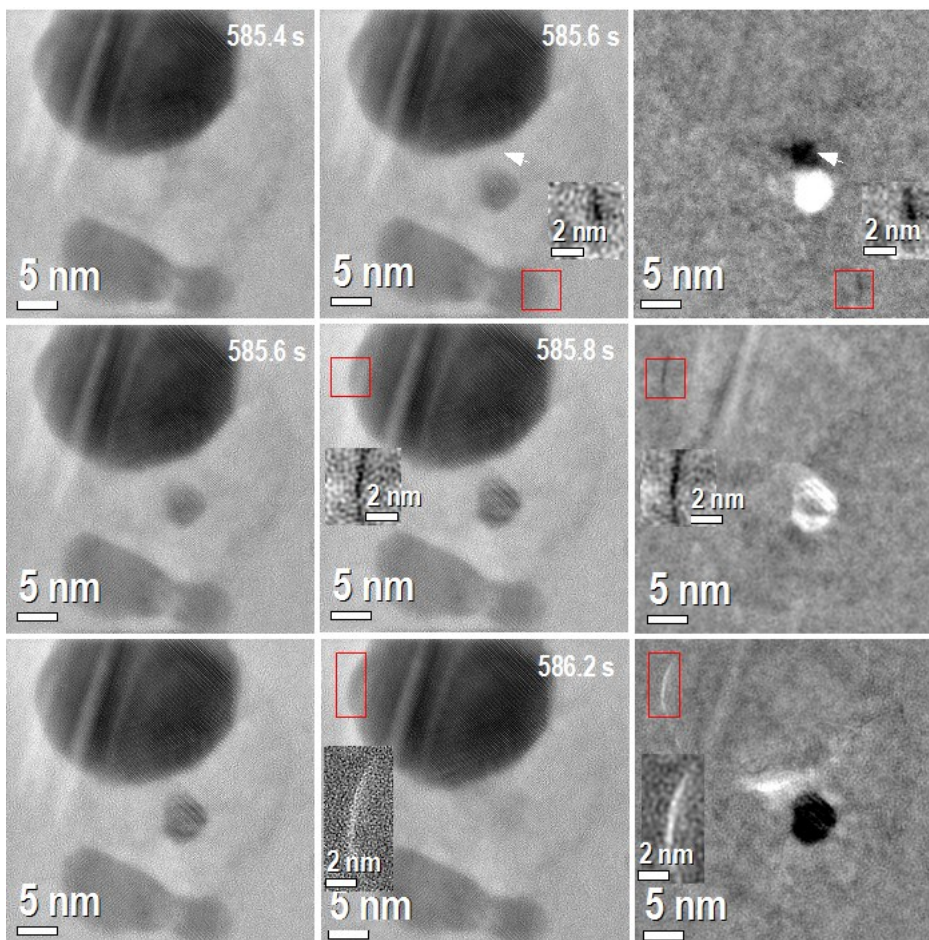


**Fig. S16.** Details of the whole process applied in the construction of Fig. 2, with the same regions highlighted by the red box and arrow.

This same process can be identified clearly in movie 1 and movie 2. Also, we showed this process in Fig. S4, S5 and S6. In Fig. S4 for example, the regions of the atoms related to the nucleation and dissolution are so easily observed that no process is necessary.

#### *AgCl thickness estimation.*

The “estimated” thickness is based on the reaction of  $\text{AgCl} + e^- \Rightarrow \text{Ag}^+ + \text{Cl}^-$ . Taking into account that the Ag atoms for growth of Ag NP on the top came from the AgCl NP and the partial dissolution of Ag NPs in the bottom. The initial areas of three Ag NPs are 298, 153, and 71 nm<sup>2</sup>. The initial volume is 5758 nm<sup>3</sup>, and the final volume (from the two final NPs) is 9083 nm<sup>3</sup>, assuming a spherical shape for all NPs. The initial area of AgCl nanoparticle is 467 nm<sup>2</sup>, and finally assuming a lamellar shape, the estimated thickness is closely 14.2 nm.